МАТЕМАТИЧНІ МЕТОДИ, МОДЕЛІ, ПРОБЛЕМИ І ТЕХНОЛОГІЇ ДОСЛІДЖЕННЯ СКЛАДНИХ СИСТЕМ

UDC 519.004.942
DOI: 10.20535/SRIT.2308-8893.2026.2.07

REGRESSION ANALYSIS OF LIGO-VIRGO OBSERVATIONS WG200115 USING CURVATURE TENSORS FROM EINSTEIN'S EQUATIONS AND DIRAC'S GRAVITATIONAL WAVES

Y. MATSUKI

Abstract. This research presents the mathematical derivation of curvature tensors from the Schwarzschild solution of the gravitational field, along with the derivation of gravitational waves as the second derivative of the field. The elimination of the event horizon is the core contribution of this paper, building on Paul Dirac's approach in his 1975 book, General Theory of Relativity. This paper introduces linear and non-linear models for the spacetime distortion function. The fit of the tensor equation for gravitational waves is tested using geometrical information from the LIGO-Virgo observation of WG200115, employing econometric techniques with indicators such as *R*-squared for the robustness of the given data and the fit of the model to the data distribution, as well as the Durbin–Watson statistic for time-series predictability. The results show a good fit of the derived mathematical model to the observed geometry. Different models for simulating spacetime distortion exhibit varying degrees of fit to the observed geometry, with a less distorted model providing a better explanation for the observed gravitational waves. The model's fit decreases when considering the rotation of the source object, whether it be a neutron star or a black hole. Further modeling effort is needed to accurately represent the NSBH merger process and its role in the formation of gravitational waves.

Keywords: curvature tensors, Schwarzschild solution, gravitational waves, event horizon, LIGO-Virgo observation.

INTRODUCTION

The Schwarzschild solution is a fundamental solution to Einstein's equations, which describes the gravitational field outside a spherical, non-rotating mass such as a black hole. However, this solution contains a singularity, or a point of infinite curvature, at a distance $r = 2m$ from the center of the black hole, known as the event horizon. The Schwarzschild metric is given by:

$$ds^2 = g_{00}dt^2 - g_{11}dr^2 - g_{22}d\theta^2 - g_{33}d\phi^2 =$$
$$= (1 - 2m/r)dt^2 - (1 - 2m/r)^{-1}dr^2 - r^2d\theta^2 - r^2\sin^2\theta d\phi^2. \quad (1)$$

Here, ds^2 represents the spacetime interval; $g_{\mu\nu}$ is the fundamental tensor of the metric; m is the mass of the black hole; and r is the distance from the center of the black hole in the radial coordinate. The diagonal elements of $g_{\mu\nu}$ are $g_{00} =$

$= (1 - 2m/r)$, $g_{11} = (1 - 2m/r)^{-1}$, $g_{22} = r^2$, and $g_{33} = r^2\sin^2\theta$, respectively in the spherical polar coordinates. Equation (1) is known as the Schwarzschild solution. It is held outside the surface of a star or black hole. [1]

To address the issue of the event horizon and extend the solution to regions where $r < 2m$, Paul Dirac proposed a transformation to a non-static coordinate system. This involves introducing new time and radial coordinates, τ and ρ, which vary with the original coordinates t and r as follows:

$$\tau = t + f(r), \tag{2}$$

$$\rho = t + g(r), \tag{3}$$

where $f(r)$ and $g(r)$ are functions of r. This transforms the Schwarzschild solution into a new form:

$$ds^2 = d\tau^2 - 2m/\{\mu(\rho - \tau)^{2/3}\}d\rho^2 - \mu^2(\rho - \tau)^{4/3}(d\theta^2 + \sin^2\theta d\phi^2). \tag{4}$$

In his 1975 book "General Theory of Relativity," Dirac also derived an equation for gravitational waves in a region of empty space, where the gravitational field is weak and the metric tensor $g_{\mu\nu}$ is approximately constant [1, p. 64]. He started with the following equation, which is applicable in such a weak gravitational field:

According to [1, p. 25, p. 27–28, p. 64], in the empty space where only the gravitational field exists, the Ricci curvature tensor $R_{\mu\nu}$ is zero:

$$R_{\mu\nu} = 0 \ . \tag{5}$$

Therefore,

$$R_{\mu\nu} = \Gamma^{\alpha}_{\mu\alpha,\nu} - \Gamma^{\alpha}_{\mu\nu,\alpha} - \Gamma^{\alpha}_{\mu\nu}\Gamma^{\beta}_{\alpha\beta} + \Gamma^{\alpha}_{\mu\beta}\Gamma^{\beta}_{\nu\alpha} = 0 \ , \tag{6}$$

where

$$\Gamma^{\alpha}_{\mu\nu} = g^{\alpha\alpha}\Gamma_{\alpha\mu\nu} = \frac{1}{2}g^{\alpha\alpha}(g_{\alpha\mu,\nu} + g_{\alpha\nu,\mu} - g_{\mu\nu,\alpha}) \ . \tag{7}$$

$R_{\mu\nu}$ is called as the Ricci tensor; $\Gamma^{\alpha}_{\mu\nu}$ is the Christoffel symbol; and $\Gamma^{\alpha}_{\mu\nu,\sigma}$ is the first derivative of the Christoffel symbol by the vector σ; $g_{\alpha\mu,\nu}$ is the first derivative of the fundamental tensor $g_{\alpha\mu}$ by the vector ν; and $g^{\alpha\alpha}$ is inverse of the fundamental tensor $g_{\alpha\alpha}$. Equation (6) shows Einstein's assumption that in empty space, the Ricci tensor is zero [1].

If the gravitational field is weak, the curvature is also weak and $g_{\mu\nu}$ is approximately constant. Therefore,

$$-\Gamma^{\alpha}_{\mu\nu}\Gamma^{\beta}_{\alpha\beta} + \Gamma^{\alpha}_{\mu\beta}\Gamma^{\beta}_{\nu\alpha} = 0 \ , \tag{8}$$

then

$$R_{\mu\nu} = \Gamma^{\alpha}_{\mu\alpha,\nu} - \Gamma^{\alpha}_{\mu\nu,\alpha} = 0 \ . \tag{9}$$

On the other hand,

$$R_{\mu\nu\rho\sigma} = \frac{1}{2}(g_{\mu\sigma,\nu\rho} - g_{\nu\sigma,\mu\rho} - g_{\mu\rho,\nu\sigma} + g_{\nu\rho,\mu\sigma}) + \Gamma_{\beta\mu\sigma}\Gamma^{\beta}_{\nu\rho} - \Gamma_{\beta\mu\rho}\Gamma^{\beta}_{\nu\sigma} \ . \tag{10}$$

Equation (10) is another expression of (6), but with the Riemann–Christoffel tensor (the curvature tensor) $R_{\mu\nu\rho\sigma}$, which is another variation of the Ricci tensor. The second term of (10) disappears in the weak gravitational field. But, in this research, it is included in the mathematical transformation to make the model of gravitational waves in the strong gravitational field, such as in the space near a black hole or a dense star.

By interchanging ρ and μ, and neglecting $\Gamma_{\beta\mu\sigma}\Gamma^{\beta}_{\nu\rho} - \Gamma_{\beta\mu\rho}\Gamma^{\beta}_{\nu\sigma}$, we get

$$R_{\mu\nu} = g^{\rho\sigma} R_{\mu\nu\rho\sigma} = g^{\rho\sigma}(g_{\rho\sigma,\mu\nu} - g_{\nu\sigma,\mu\rho} - g_{\mu\rho,\nu\sigma} + g_{\mu\nu,\rho\sigma}) = 0. \quad (11)$$

Then

$$g^{\mu\nu}(g_{\mu\nu,\rho\sigma} - g_{\mu\rho,\nu\sigma} - g_{\mu\sigma,\nu\rho} + g_{\rho\sigma,\mu\nu}) = 0. \quad (12)$$

On the other hand, the moving particle in a scalar field of the potential energy V follows d'Alembert equation,

$$\nabla V = g^{\mu\nu}(V_{,\mu\nu} - \Gamma^{\alpha}_{\mu\nu} V_{,\alpha}) = 0 \ . \quad (13)$$

In order to describe a particle moving in the 4-dimensional time-space, V is replaced by vectors x^{λ} of the 4-dimensional coordinates in which $x^{\lambda}{}_{,\alpha} = g^{\lambda}{}_{\alpha}$, then d'Alembert equation becomes

$$g^{\mu\nu} g^{\lambda}_{\alpha,\nu} - g^{\mu\nu} g^{\lambda}_{\alpha} \Gamma^{\alpha}_{\mu\nu} = 0 \ . \quad (14)$$

Then

$$g^{\mu\nu} \Gamma^{\lambda}_{\mu\nu} = 0 \ . \quad (15)$$

Meanwhile,

$$\Gamma^{\lambda}_{\mu\nu} = g^{\lambda\rho} \Gamma_{\rho\mu\nu} = \frac{1}{2} g^{\lambda\rho}(g_{\rho\mu,\nu} + g_{\rho\nu,\mu} - g_{\mu\nu,\rho}) \ . \quad (16)$$

So,

$$g^{\mu\nu}\Gamma^{\lambda}_{\mu\nu} = \frac{1}{2} g^{\lambda\rho} g^{\mu\nu}(g_{\rho\mu,\nu} + g_{\rho\nu,\mu} - g_{\mu\nu,\rho}) = g^{\lambda\rho} g^{\mu\nu}(g_{\rho\mu,\nu} - \frac{1}{2} g_{\mu\nu,\rho}) = 0 \ , \quad (17)$$

where

$$g_{\rho\nu,\mu} = y_{n,\rho\mu} y^{n}_{,\nu} + y_{n,\nu\mu} y^{n}_{,\rho} = y_{n,\rho\nu} y^{n}_{,\mu} + y_{n,\mu\nu} y^{n}_{,\rho} = g_{\rho\mu,\nu} \ , \quad (18)$$

where μ and ν are in symmetrical relation in the equation, therefore they are exchangeable; and

$$y^{n}_{,\mu} = \frac{\partial y^{n}(x^{\mu})}{\partial x^{\mu}} \ , \quad (19)$$

where μ = 0, 1, 2, 3, while x^{μ}, a vector in μ-th dimension, is located in the N-dimensional physical space of y^{n}, n = 1, 2, .., N.

Therefore,

$$g^{\mu\nu}(g_{\rho\mu,\nu} - \frac{1}{2} g_{\mu\nu,\rho}) = 0 \ . \quad (20)$$

Then, in order to describe the waves moving in the gravitational field, it is differentiated by x^{σ}.

$$\frac{d}{dx^{\sigma}} g^{\mu\nu}(g_{\rho\mu,\nu} - \frac{1}{2} g_{\mu\nu,\rho}) = g^{\mu\nu}_{,\sigma}(g_{\rho\mu,\nu} - \frac{1}{2} g_{\mu\nu,\rho}) + g^{\mu\nu}(g_{\mu\rho,\nu\sigma} - \frac{1}{2} g_{\mu\nu,\rho\sigma})$$
$$= g^{\mu\nu}(g_{\mu\rho,\nu\sigma} - \frac{1}{2} g_{\mu\nu,\rho\sigma}) = 0 \ . \quad (21)$$

In the equation (17),

$$g^{\lambda\rho} g^{\mu\nu} \left(g_{\rho\mu,\nu} - \frac{1}{2} g_{\mu\nu,\rho} \right) = 0 \ . \quad (22)$$

because $g_{\rho\mu}$ is approximately constant in the weak gravitational field. Therefore,

$$g_{\rho\mu,\nu} = 0 \ . \quad (23)$$

By interchanging ρ and σ of (21),

$$g^{\mu\nu}(g_{\mu\sigma,\nu\rho} - \frac{1}{2}g_{\mu\nu,\sigma\rho}) = g^{\mu\nu}(g_{\mu\sigma,\nu\rho} - \frac{1}{2}g_{\mu\nu,\rho\sigma}) = 0 \ . \tag{24}$$

By adding (12), (21) and (22), we get

$$g^{\mu\nu}g_{\rho\sigma,\mu\nu} = 0 \ . \tag{25}$$

This satisfies the d'Alembert equation, describing waves propagating at the speed of light in empty space with a weak gravitational field. It is noted that gravitational waves are mathematically expressed as the second derivatives of the gravitational field tensor. [1]

HIGHLIGHTS OF THIS RESEARCH PAPER

While Dirac's work derived gravitational waves in the weak gravitational field, the novelty of this research lies in deriving gravitational waves in a strong gravitational field, where the metric tensor is not constant, as opposed to a weak one. Econometric techniques [2] are then applied to assess how well these tensors fit the observational data from the **LIGO-Virgo Collaboration**, a global scientific collaboration dedicated to detecting gravitational waves, with a particular focus on the WG200115 event [3] This approach incorporates both linear and non-linear models of spacetime distortion to evaluate their effectiveness in explaining the observed gravitational waves. GW200115 was identified as a compact binary coalescence candidate by multiple low-latency matched-filtering pipelines in LIGO Hanford and LIGO Livingston. The event was detected on January 15, 2020, at 04:23:10 UTC and was significant enough to be reported within six minutes. The initial sky map indicated a 90 % credible region of 900 square degrees, providing a spatial localization of the event in the sky. This rich data set, including the precise detection time and well-defined sky map, offers a reliable basis for evaluating the fit of the derived mathematical models to the observed geometry of gravitational waves.

NOVEL TENSOR EQUATION OF GRAVITATIONAL WAVES IN STRONG CURVATURE

The following derivations extend beyond what Dirac covered in his publication. The equation (25) describes waves moving in a weak gravitational field that approximates a flat 4-dimensional spacetime. However, to accurately predict the behavior of these waves, it is essential to describe them in curvilinear coordinates within stronger gravitational fields at their source, as the waves are formed from the movement of compact objects with significant mass.

By ensuring our model transitions smoothly from the strong gravitational field at the source to the nearly flat field during propagation to detectors such as LIGO and Virgo, we provide a comprehensive representation of gravitational waves' behavior. This approach allows us to accurately simulate both the emission of the waves in a strong gravitational field and their travel through the universe, where the spacetime curvature is much weaker. This comprehensive model negates the need for separate simulations for different curvature regimes, provided it can be validated against known weak-field results.

To simulate the flow of waves coming from a stronger gravitational field, the following terms are necessary [6–8], which were neglected by Dirac [1, pp. 27–28, p. 64]:

$$-\Gamma^{\alpha}_{\mu\nu}\Gamma^{\beta}_{\alpha\beta}+\Gamma^{\alpha}_{\mu\beta}\Gamma^{\beta}_{\nu\alpha}\neq 0 \tag{26}$$

for the equation (8),

$$\Gamma_{\beta\mu\sigma}\Gamma^{\beta}_{\nu\rho}-\Gamma_{\beta\mu\rho}\Gamma^{\beta}_{\nu\sigma}\neq 0 \tag{27}$$

for the neglected last two terms in the equation (10), and

$$g^{\lambda\rho}g^{\mu\nu}\left(g_{\rho\mu,\nu}-\frac{1}{2}g_{\mu\nu,\rho}\right)=0 \tag{28}$$

for the equation (22).

The equations below from (29) to (33) show the same process from (20) to (25) that derive the equation of the waves in the approximation of the curvilinear coordinates, but the equations below include those neglected terms in order to derive them in curvilinear coordinates. By including the neglected terms into the equation (20), we get:

$$\begin{aligned}
R_{\mu\nu}&=g^{\rho\sigma}R_{\mu\nu\rho\sigma}=g^{\rho\sigma}(g_{\rho\sigma,\mu\nu}-g_{\nu\sigma,\mu\rho}-g_{\mu\rho,\nu\sigma}+g_{\mu\nu,\rho\sigma})+g^{\rho\sigma}\Gamma_{\beta\rho\sigma}\Gamma^{\beta}_{\mu\nu}-g^{\rho\sigma}\Gamma_{\beta\mu\rho}\Gamma^{\beta}_{\nu\sigma}\\
&=g^{\rho\sigma}(g_{\rho\sigma,\mu\nu}-g_{\nu\sigma,\mu\rho}-g_{\mu\rho,\nu\sigma}+g_{\mu\nu,\rho\sigma})+g^{\rho\sigma}g_{\beta\beta}\Gamma_{\beta\rho\sigma}\Gamma_{\beta\mu\nu}-g^{\rho\sigma}g_{\beta\beta}\Gamma_{\beta\mu\rho}\Gamma_{\beta\nu\sigma}\\
&=g^{\rho\sigma}(g_{\rho\sigma,\mu\nu}-g_{\nu\sigma,\mu\rho}-g_{\mu\rho,\nu\sigma}+g_{\mu\nu,\rho\sigma})\\
&\quad+g^{\rho\sigma}g_{\beta\beta}\frac{1}{2}(g_{\beta\rho,\sigma}+g_{\beta\sigma,\rho}-g_{\rho\sigma,\beta})(g_{\beta\mu,\nu}+g_{\beta\nu,\mu}-g_{\mu\nu,\beta})\\
&\quad-g^{\rho\sigma}g_{\beta\beta}\frac{1}{2}(g_{\beta\mu,\rho}+g_{\beta\rho,\mu}-g_{\mu\rho,\beta})(g_{\beta\nu,\sigma}+g_{\beta\sigma,\nu}-g_{\nu\sigma,\beta})\\
&=g^{\rho\sigma}(g_{\rho\sigma,\mu\nu}-g_{\nu\sigma,\mu\rho}-g_{\mu\rho,\nu\sigma}+g_{\mu\nu,\rho\sigma})+(\frac{1}{2}g^{\rho\sigma}g_{\beta\beta}g_{\rho\sigma,\beta}g_{\nu\sigma,\beta})=0\,.
\end{aligned} \tag{29}$$

Interchanging ρ, μ, σ and ν, we get

$$g^{\mu\nu}(g_{\mu\nu,\rho\sigma}-g_{\mu\rho,\nu\sigma}-g_{\mu\sigma,\nu\rho}+g_{\rho\sigma,\mu\nu})+(\frac{1}{2}g^{\rho\mu}g_{\beta\beta}g_{\rho\mu,\beta}g_{\nu\mu,\beta})=0\,. \tag{30}$$

By including the neglected terms into the equation (30), we get

$$\begin{aligned}
&\frac{d}{dx^{\sigma}}\{g^{\mu\nu}(g_{\rho\mu,\nu}-\frac{1}{2}g_{\mu\nu,\rho})+\frac{1}{2}g^{\rho\mu}g_{\beta\beta}g_{\rho\mu,\beta}g_{\mu\nu,\beta}\}\\
&=g^{\mu\nu}_{,\sigma}(g_{\rho\mu,\nu}-\frac{1}{2}g_{\mu\nu,\rho})+g^{\mu\nu}(g_{\mu\rho,\nu\sigma}-\frac{1}{2}g_{\mu\nu,\rho\sigma})+(\frac{1}{2}g^{\rho\mu}g_{\beta\beta}g_{\rho\mu,\beta}g_{\nu\mu,\beta\sigma})+(\frac{1}{2}g^{\rho\mu}g_{\beta\beta}g_{\rho\mu,\beta\sigma}g_{\nu\mu,\beta})\\
&\quad+(\frac{1}{2}g^{\rho\mu}_{,\sigma}g_{\beta\beta}g_{\rho\mu,\beta}g_{\nu\mu,\beta})+(\frac{1}{2}g^{\rho\mu}g_{\beta\beta,\sigma}g_{\rho\mu,\beta}g_{\nu\mu,\beta})=0\,.
\end{aligned} \tag{31}$$

Interchanging ρ and σ in (31), we get

$$\begin{aligned}
&=g^{\mu\nu}_{,\rho}(g_{\sigma\mu,\nu}-\frac{1}{2}g_{\mu\nu,\sigma})+g^{\mu\nu}(g_{\mu\sigma,\nu\rho}-\frac{1}{2}g_{\mu\nu,\sigma\rho})+(\frac{1}{2}g^{\sigma\mu}g_{\beta\beta}g_{\sigma\mu,\beta}g_{\nu\mu,\beta\rho})+(\frac{1}{2}g^{\sigma\mu}g_{\beta\beta}g_{\sigma\mu,\beta\rho}g_{\nu\mu,\beta})\\
&\quad+(\frac{1}{2}g^{\sigma\mu}_{,\rho}g_{\beta\beta}g_{\sigma\mu,\beta}g_{\nu\mu,\beta})+(\frac{1}{2}g^{\sigma\mu}g_{\beta\beta,\rho}g_{\sigma\mu,\beta}g_{\nu\mu,\beta})=0\,.
\end{aligned} \tag{32}$$

Adding (30), (31) and (32), we get

$$g^{\mu\nu}{}_{\rho\sigma,\mu\nu}+g^{\mu\nu}_{,\sigma}(g_{\rho\mu,\nu}-\frac{1}{2}g_{\mu\nu,\rho})+g^{\mu\nu}_{,\rho}(g_{\sigma\mu,\nu}-\frac{1}{2}g_{\mu\nu,\sigma})$$

$$+\frac{1}{2}g^{\rho\mu}g_{\beta\beta}g_{\rho\mu,\beta}g_{\nu\mu,\beta\sigma}+\frac{1}{2}g^{\rho\mu}g_{\beta\beta}g_{\rho\mu,\beta\sigma}g_{\nu\mu,\beta}$$

$$+\frac{1}{2}g^{\rho\mu}_{,\sigma}g_{\beta\beta}g_{\rho\mu,\beta}g_{\nu\mu,\beta}+\frac{1}{2}g^{\rho\mu}g_{\beta\beta,\sigma}g_{\rho\mu,\beta}g_{\nu\mu,\beta}$$

$$+\frac{1}{2}g^{\sigma\mu}g_{\beta\beta}g_{\sigma\mu,\beta}g_{\nu\mu,\beta\rho}+\frac{1}{2}g^{\sigma\mu}g_{\beta\beta}g_{\sigma\mu,\beta\rho}g_{\nu\mu,\beta}$$

$$+\frac{1}{2}g^{\sigma\mu}_{,\rho}g_{\beta\beta}g_{\sigma\mu,\beta}g_{\nu\mu,\beta}+\frac{1}{2}g^{\sigma\mu}g_{\beta\beta,\rho}g_{\sigma\mu,\beta}g_{\nu\mu,\beta}=0. \quad (33)$$

Numbers, 0, 1, 2 and 3 are assigned to each of μ, ν, ρ, σ and β of (33); then by the rule of tensor, all terms are summed up. The actual functions of the curvature tensors are derived from the diagonal elements, g_{00}, g_{11}, g_{22}, and g_{33}, of equation (4). Also,

If $\beta = \rho$, $g^{\rho\mu}g_{\beta\beta}g_{\rho\mu,\beta}g_{\nu\mu,\beta\sigma} = g^{\rho\mu}g_{\rho\rho}g_{\rho\nu,\rho}g_{\nu\mu,\rho\sigma}$.

Then if $\mu = \rho$, $g^{\rho\mu}g_{\rho\rho} = g^{\mu}_{\rho} = 1$.

And if $\mu \neq \rho$, $g^{\rho\mu}g_{\rho\rho} = g^{\mu}_{\rho} = 0$.

If $\mu = \rho = \beta$, $g^{\rho\mu}_{,\sigma} \cdot g_{\beta\beta} \neq 0$.

But if not $\mu = \rho = \beta$, $g^{\rho\mu}_{,\sigma} \cdot g_{\beta\beta} = 0$.

And also, if $\mu = \rho = \beta$, $g^{\rho\mu}g_{\beta\beta,\sigma} \neq 0$.

But if not $\mu = \rho = \beta$, $g^{\rho\mu}g_{\beta\beta,\sigma} = 0$.

All the derived elements of gravitational waves are shown in Appendix 1 Curvature tensors of gravitational waves. If the simulation of gravitational waves is conducted, focusing their spatial distribution, not on the time distribution in the 4-dimensional time-space, the element for $\mu = \nu = 0$ is excluded from the simulation, and then only the following diagonal elements of a 3 by 3 matrix are considered:

For $\mu = \nu = 1$,

$$W_{11} = \frac{16}{9(\rho-\tau)^2} + \frac{8}{3(\rho-\tau)^2} + \frac{64m}{27\mu(\rho-\tau)^{\frac{11}{3}}} - \frac{144m}{27\mu(\rho-\tau)^{\frac{13}{3}}} + \frac{8\mu^3}{9m}\sin^2\theta + \frac{16\mu^3}{18m}. \quad (34)$$

For $\mu = \nu = 2$,

$$W_{22} = 8\cos^2\theta - 8\sin^2\theta. \quad (35)$$

For $\mu = \nu = 3$,

$$W_{33} = \frac{128}{9(\rho-\tau)^2} + 16\cot^2\theta. \quad (36)$$

HAMILTONIAN LIKE APPROACH FOR REGRESSION ANALYSIS

The next step is the derivation of gravitational waves emitted from a rotating black hole. First, the following 3 by 3 matrix from (34), (35) and (36) are formulated:

$$W_{\mu\nu} = W_{11} + W_{22} + W_{33} = c_1X_1 + c_2X_2 + c_3X_3 \quad (37)$$

The stress energy tensor, T, reflects the energy intensities of the waves, where k is a constant.

$$W_{\mu\nu} = kT \quad (38)$$

Then each of the coefficients of (37) relates to the elements of the waves such as $1/(\rho-\tau)^{-2}$, $1/(\rho-\tau)^{-3/11}$, and so on. This is not Hamiltonian, but form of the equation

as well as calculations of the coefficients resonate the Hamiltonian equation of motion in the perturbation theory in quantum mechanics.

GRAVITATIONAL WAVES FROM A ROTATING BLACK HOLE

For derive the tensor equation, Euler angles (39) [4, pp.150–154] is multiplied to (38).

$$D = \begin{bmatrix} \cos\phi & \sin\phi & 0 \\ -\sin\phi & \cos\phi & 0 \\ 0 & 0 & 1 \end{bmatrix} \tag{39}$$

This operation results (40).

$$D \cdot W_{\mu\nu} = \begin{pmatrix} \cos\varphi & \sin\varphi & 0 \\ -\sin\varphi & \cos\varphi & 0 \\ 0 & 0 & 1 \end{pmatrix} \cdot \begin{bmatrix} W_{11} & 0 & 0 \\ 0 & W_{22} & 0 \\ 0 & 0 & W_{33} \end{bmatrix} = \begin{bmatrix} \cos\varphi \cdot W_{11} & \sin\varphi \cdot W_{22} & 0 \\ -\sin\varphi \cdot W_{11} & \cos\varphi \cdot W_{22} & 0 \\ 0 & 0 & W_{33} \end{bmatrix} \tag{40}$$

With the next equation (41), the coefficients, c_1, c_2, ⋯ and c_6 are calculated for the energy intensity of the gravitational waves emitted from a black hole that rotates.

$$c_1 \frac{1}{(\rho - \tau)^2} + c_2 \frac{1}{(\rho - \tau)^{\frac{11}{3}}} + c_3 \frac{1}{(\rho - \tau)^{\frac{13}{3}}} + c_4 \sin^2\theta + c_5(\cos^2\theta - \sin^2\theta) + c_6 \cot^2\theta = kT \tag{41}$$

where T is a stress-energy tensor, which is explained below; and k is a constant value, which is 1 in this research. The equation (41) is non-linear, however in this simulation, all variables are assigned by the inputdata, which have been calculated in advance as shown in the following section. Therefore, each term has a coefficient and variable, then the coefficient is calculated by linear-regression analysis.

GEOMETRIC DATA FROM WG200115 OBSERVATION FOR NUMERIC SIMULATION

Event **GW200115**, detected on **January 15, 2020, at 04:23:10 UTC**, was observed at a **luminosity distance** of **300 Mpc** from Earth. This distance is a measure of how far the event is, based on the brightness of the gravitational wave signal. Additionally, the event exhibited a **spin magnitude with a negative spin projection**, meaning the spin of the primary object (likely the black hole) was oriented opposite to the orbital angular momentum of the binary system.

These values are integrated at appropriate points in Table 1, while maintaining the overall structure across 25 grid points. The table reflects the luminosity distance (r) ranging from 0 to 300 Mpc to encompass the observed values, with θ (theta) and ϕ (phi) values derived from typical ranges for these angles in spherical coordinates. For simplicity, θ ranges from 0 to π, and ϕ ranges from 0 to 2π.

In the context of simulating gravitational wave detections from sources like GW200115, observed by LIGO and Virgo, it's essential to align the theoretical model's timescale with the practical detection window. The timescale depicted in Fig. 1 and Table 1 spans from 0 to approximately 3.15×10^7 seconds, corresponding to the light travel time over a cosmological distance of 300 Mpc (megaparsecs).

Given that 1 Mpc equals 3.086×10^{22} meters, the total distance of 300 Mpc is 9.258×10^{24} meters. Using the speed of light (3×10^{8} meters per second), the calculated light travel time is approximately $3.086\times10^{24}\div3\times10^{8}=1.029\times10^{16}$ seconds, or about 326 million years.

The reported distance to the source is the distance from the Earth to the region in the sky where the source is likely located. This distance comes with an uncertainty range. The detected area in the sky (with 90% probability) indicates the location but not the precise point of the spinning neutron star-black hole (NSBH) system or other source.

For the calculations, the time and distance values over 25 grid points are converted into logarithm, in order to use the statistical software tool, SST.

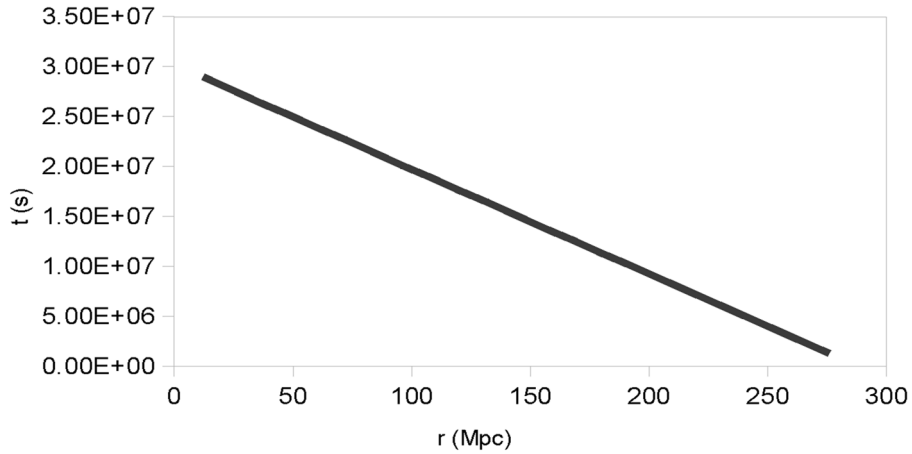

Fig. 1. Time and distance taken from geometric data from WG200115

The polar angle (θ) can be interpreted from the sky localization data provided by the gravitational wave observations. This data is typically available in the form of sky maps with credible regions indicating the probable location of the source. However, the goal of this simulation is to perform a general simulation to explore the overall behavior of gravitational waves in a broad sense expressed by the curvature tensor equation, by investigating the fitting of the equation in a possible geometry between observable gravitational waves and the ground observatories such as LIGO-Virgo observatories. Therefore, the input data set is chosen as: r ranging from 0 to 300 Mpc (to include the observed values), and θ and ϕ values derived from typical ranges for these angles in spherical coordinates. For simplicity, it was assumed θ ranges from 0 to π.

The azimuthal angle (ϕ) is related to the rotational orientation of the system. This can often be cyclic, meaning it repeats over a 360-degree range. For this study, a distribution was assumed, based on the characteristics of the system. For a rotating black hole in an NSBH system, the azimuthal angle could be inferred from the angular momentum vector orientation or other related parameters. However, the curvature tensor equation (41) doesn't model the binary system such as NSBH, in which there are individual object's spin as well as the orbit rotation. Therefore, we assumed as if one object rotates, to examine how rotation may generally influence the fitting of the derived curvature tensor equation. And it was assumed ϕ ranges from 0 to 2π, which is a single cycle of the rotation during the time period of the

light travels from the observed gravitational waves to the LIGO-Virgo observatories.

Fig. 2 shows the values of θ and ϕ over the 23 discrete r values for a single cycle.

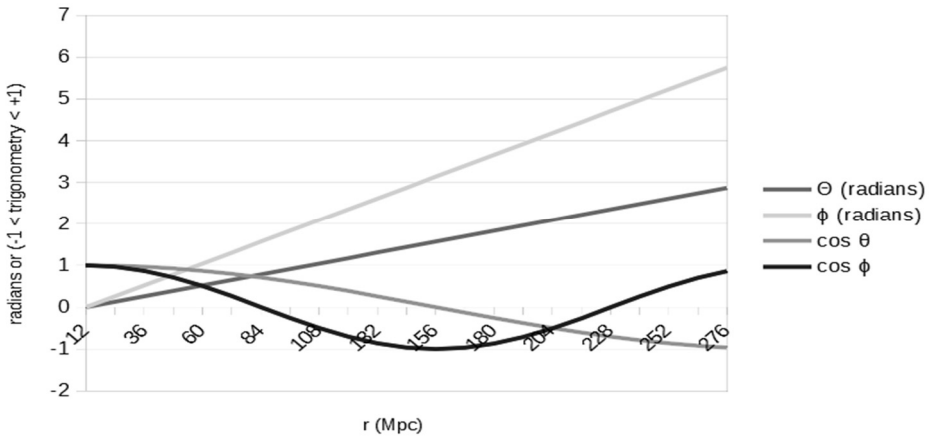

Fig. 2. Values of θ, ϕ, cos θ and cos ϕ

CONSTRUCTION OF THE DEPENDENT VARIABLE FOR THE REGRESSION

The dependent variable for the regression to evaluate the fitting of the model in the data taken from the observation is constructed by the stress energy tensor of the Einstein's field equation [4]. The stress energy tensor in 4-dimensional space time is:

$$T^{\mu\nu} = \begin{bmatrix} \rho & 0 & 0 & -\frac{J}{r^2} \\ 0 & p_r & 0 & 0 \\ 0 & 0 & p_\theta & 0 \\ -\frac{J}{r^2} & 0 & 0 & p_\phi \end{bmatrix}, \tag{42}$$

where ρ is energy density; J is angular momentum of the rotation of the emission source; r is distance; p_r, p_θ, p_ϕ are pressures of the waves (which might be zero or negligible in vacuum) [5]. In this simulation, only spacial elements are considered as shown in (43):

$$T^{\mu\nu} = \begin{bmatrix} p_r & 0 & 0 \\ 0 & p_\theta & 0 \\ 0 & 0 & p_\phi \end{bmatrix}. \tag{43}$$

In regions far from the black hole where the gravitational waves are detected, the pressures might be very small but not exactly zero. As typically in a vacuum solution (black hole exterior), these elements, p_r, p_θ, p_ϕ, are negligible, but in order to calculate the coefficients of the regress-able equations, very small values are used as shown in Fig. 3 and Table 1 are considered as the effects of surrounding field.

However, because this analysis focuses on the space coordinates, r, θ and ϕ, excluding the time coordinates, the dependent variable is the sum of the sum the three pressure values p_r, p_θ, and p_ϕ to create a single dependent variable Y for the regression model. This approach simplifies the tensor/matrix form into a scalar equation that can be handled using standard regression techniques. Evaluation of the fitting of the model is made by assessing the significance of each coefficient (e.g., using p-values) and the overall fit of the model (e.g., using R^2).

POSSIBLE VALUES FOR PRESSURES

For the simulation small, non-zero values for the pressures are assumed for the sake of your regression analysis.

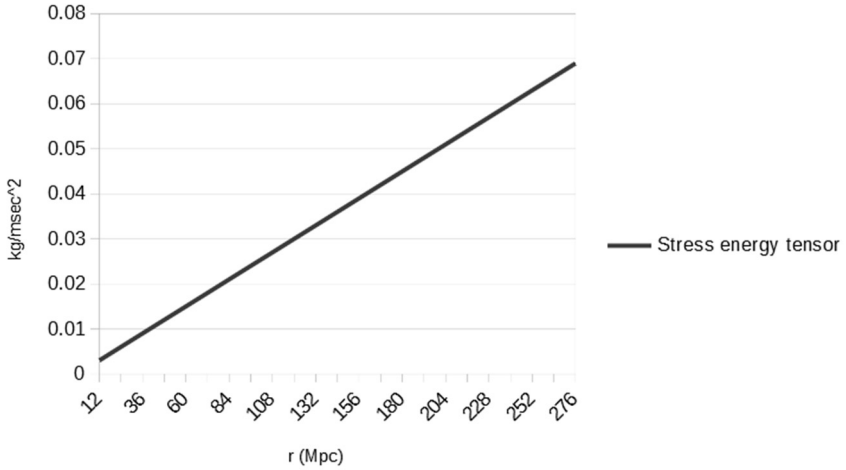

Fig. 3. Values of Stress Energy Tensor

Table 1. Input data (1/2)

r (Mpc)	t (sec)	τ, linear	τ, non-linear	ρ, linear	ρ, non-linear
0	0	0	0	0	0
12	2.90e+07	2.90e+07	2.90e+07	2.90e+07	2.92e+07
24	2.77e+07	2.77e+07	2.77e+07	2.77e+07	2.65e+10
36	2.64e+07	2.64e+07	2.64e+07	2.64e+07	4.31e+15
48	2.52e+07	2.52e+07	2.52e+07	2.52e+07	7.02e+20
...	...	...	...	...	...
276	1.26e+06	1.26e+06	1.26e+06	1.26e+06	7.33e+119

Table 1. Input data (2/2)

r (Mpc)	Θ (radians)	ϕ (radians)	p_r	p_θ	p_ϕ
0	0	0	0	0	0
12	0.13	0.26	0.001	0.001	0.001
24	0.26	0.52	0.002	0.002	0.002
36	0.39	0.78	0.003	0.003	0.003
48	0.52	1.04	0.004	0.004	0.004
...	...	...	...	...	...
276	3.00	6.01	0.025	0.025	0.025

MODELS FOR SPACE TIME DISTORTION

For spacetime distortion models, each of $f(r)$ and $g(r)$ shown in (2) and (3) was given by linear distortion model and non-linear distortion model as shown in Table 2. The values of distorted spacetime, τ and ρ, are shown in Table 2.

Table 2. Two models for simulating the distorted time-space

	Case-1 (Non-linear model)	**Case-2 (Linear model)**
$f(r)$	$log{\cdot}r$	$1/r$
$g(r)$	e^r	r

RESULT

The coefficients of equations (38) and (41), as well as the R-squared values and Durbin–Watson statistics, were calculated using SST, a statistical software developed by Jeffrey Dubin and Douglas Rivers at Caltech in 1986 with the assistance of several Caltech students. The coefficients represent the strength of each term in the equations. These values are accompanied by the standard errors of the estimated coefficients and the corresponding t-statistics. t-statistics are calculated by dividing the coefficient value by its standard error; higher t-statistics indicate greater statistical significance of the coefficient. After establishing statistical significance, the magnitude of the coefficient itself reflects the comparative strength of each term in the equation. If one or more statistically significant coefficients are larger than others, these terms have a greater influence on the stress-energy tensor, which reflects the energy intensity on the right-hand side of the equation and consists of the terms, i.e., independent variables, in regression analysis.

The R-squared value, as calculated using equation (44), indicates how well the model explains the observed data related to the geometry of gravitational waves. It ranges from 0 to 1.0, with a value of 1.0 signifying a perfect fit to the observed data, while values between 0 and 1.0 represent varying degrees of fit. The objective of this report is to determine which terms in equations (38) and (41) are most influential on the stress-energy tensor and to evaluate which model—linear or nonlinear for spacetime distortion, and whether including or excluding rotation of the emission source—best explains the observed gravitational wave phenomena.

$$R^2 = \frac{\sum_i (\hat{y}_i - \bar{y})^2}{\sum_i (y_i - \bar{y})^2}, \tag{44}$$

where y_i is the i-th value of the dependent variable; $\hat{y}_i$ is called the expected value, which is the calculated i-th value of the dependent variable upon the obtained formula (37), where $y = kT$ of (38); and $\bar{y}$ is the average value of the dependent variable y.

The Durbin–Watson statistic, as defined by equation (45), measures the degree to which the current value of a variable can be predicted based on its previous value. A Durbin–Watson statistic value close to 2.0 suggests that the immediate future

values can be predicted well by the immediate past values, indicating a well-behaved model. Conversely, values significantly less than 2.0 suggest that past values may not effectively predict future values. This indicates that the model might not fully account for the time-dependency or spatial relationship in the data, potentially affecting the accuracy of the predictions.

$$2(1-\hat{\rho}), \tag{45}$$

where

$$\hat{\rho} = \sum_{i=2}^{n} e_i e_{i-1} / \sum_{i=2}^{n} e_{i-1}^2, \tag{46}$$

$$e_i = y_i - \hat{y}, \tag{47}$$

$$i = 1,2,....23. \tag{48}$$

All estimated coefficients are shown in Appendices from 2–1 to 2–4. Table 3 presents the tensor terms that hold statistically significant and relatively large estimated coefficients, along with *R*-squared values and Durbin–Watson statistics for cases involving linear spacetime distortion with and without the source's rotation, as well as non-linear spacetime distortion without rotation. For non-linear distortion with rotation, SST detected correlations between the independent variables, resulting in the termination of the calculation process. Consequently, for this case, the coefficients' values, the *R*-squared value and Durbin–Watson statistics were calculated manually using SST's manual mode.

Table 4 displays the independent variables with statistically and relatively significant estimated coefficients, standard errors, and *t*-statistics for gravitational waves in the linear spacetime distortion model without assuming source rotation. Table 5 presents data for the linear spacetime distortion model with source rotation, while Table 6 shows results for the non-linear spacetime distortion model without source rotation. For the non-linear spacetime distortion model with source rotation, standard errors and *t*-statistics were not obtained using SST, and manual calculations were not performed as this case appeared to be irrelevant to this report. However, the manually calculated coefficient values, *R*-squared value, and Durbin–Watson statistics for this case are shown in Appendix 2–4.

In the linear spacetime distortion model, the *R*-squared value is higher without rotation, indicating a better fit to the geometric information of the observed gravitational waves when the source's rotation is not assumed. However, the Durbin–Watson statistic is closer to the ideal value of 2.0 when rotation is assumed, suggesting that the gravitational waves exhibit smoother behavior over spacetime distribution with rotation. For the non-linear spacetime distortion model, only the no-rotation case provides meaningful results with the *R*-squared value comparable to the linear model, but the Durbin–Watson statistic is less informative, at 0.75492. When rotation is assumed, the analysis yields no meaningful results, as the *R*-squared value becomes excessively large and the Durbin–Watson statistic too small as shown in Table 3. These findings suggest that the spacetime between the observed gravitational waves and the Earth observatory is better represented by the linear spacetime distortion model than the non-linear model.

Tables 7 and 8 compare the correlations of the independent variables in the linear and non-linear models, both with the assumption of source rotation. The non-

linear model shows more correlations among the independent variables than the linear model, which led to SST terminating its operation for the non-linear case due to these correlations.

Figs. 4 and 5 compare the stress-energy tensor as the input data for the dependent variable with the predicted dependent variable after calculating the coefficient values in both the linear and non-linear models. The non-linear case exhibits anomalies in the predicted dependent variable near the location of the gravitational waves, resulting in an extremely poor *R*-squared value and a low Durbin–Watson statistic (Table 3).

Regarding the terms in the tensor equations, trigonometric functions are influential in the linear model, while spacetime functions become influential in the non-linear model when source rotation is not assumed.

Table 3. Significant independent variables, *R*-Squared and Durbin–Watson statistics

	Tensor terms with statistically significant and larger coefficients	***R*-squared**	**Durbin–Watson statistics**
No rotation, linear space time distortion	$\sin^2\theta$	0.95030	1.18063
Rotation, linear space time distortion	$\cot^2\theta$	0.78633	1.87168
No rotation, non-linear spacetime distortion	$\frac{1}{(\rho-\tau)^2}$, $\sin^2\theta$, $\frac{1}{(\rho-\tau)^{\frac{13}{3}}}$, $\cos^2\theta - \sin^2\theta$	0.95736	0.75429
Non-Linear – Rotation	SST stopped the analysis, due to the correlations between the independent variables	6.05462e+002 (Manually calculated)	0.32756 (Manually calculated)

Table 4. No rotation, linear space time distortion

Selected Independent Variable	**Estimated Coefficient**	**Standard Error**	***t*-statistic**
$\sin^2\theta$	0.10526	3.59601e-003	29.27186

Table 5. Rotation, linear space time distortion

Selected Independent Variable	**Estimated Coefficient**	**Standard Error**	***t*-statistic**
$\cos\varphi \sin^2\theta$	-5.09843e-002	5.09539e-003	-10.00596
$\cos\varphi (\cos^2\theta - \sin^2\theta)$	-9.87054e-003	8.15690e-003	-1.21008
$\cot^2\theta$ *	5.17654e-002	5.10418e-003	10.14176

Table 6. No rotation, non-linear spacetime distortion

Selected Independent Variable	Estimated Coefficient	Standard Error	*t*-statistic
$\frac{1}{(\rho-\tau)^2}$	1.22587	0.32131	3.81529
$\frac{1}{(\rho-\tau)^{\frac{13}{3}}}$	-0.68259	4.58014e-002	-14.90334
$\sin^2\theta$	0.26481	1.38169e-002	19.16566
$\cos^2\theta - \sin^2\theta$	0.13871	8.71783e-003	15.91077

Table 7. Correlations of the independent variables
(Linear spacetime distortion with rotation of the emission source)

	$\cos\phi/(\rho-\tau)^2$	$\cos\phi/(\rho-\tau)^{11/3}$	$-\cos\phi/(\rho-\tau)^{13/3}$	$\cos\phi\sin^2\theta$	$\cos\phi\ (\cos^2\theta-\sin^2\theta)$	$1/(\rho-\tau)^2$
$\cos\phi/(\rho-\tau)^{11/3}$	0.99499					
$-\cos\phi/(\rho-\tau)^{13/3}$	-3.80095e-002	-3.80696e-002				
$\cos\phi\sin^2\theta$	7.10911e-002	6.82249e-002	0.73498			
$\cos\phi\ (\cos^2\theta-\sin^2\theta)$	0.11066	0.13808	0.28929	0.43686		
$1/(\rho-\tau)^2$	0.98018	0.96950	-6.85755e-002	1.51910e-002	2.84118e-002	
$\cot^2\theta$	7.14286e-002	6.85684e-002	0.73603	1.00000	0.43675	1.56263e-002

Table 8. Correlations of the independent variables
(Non-linear spacetime distortion with rotation of the emission source)

	$\cos\phi/(\rho-\tau)^2$	$\cos\phi/(\rho-\tau)^{11/3}$	$-\cos\phi/(\rho-\tau)^{13/3}$	$\cos\phi\sin^2\theta$	$\cos\phi\ (\cos^2\theta-\sin^2\theta)$	$1/(\rho-\tau)^2$
$\cos\phi/(\rho-\tau)^{11/3}$	1.00000					
$-\cos\phi/(\rho-\tau)^{13/3}$	-0.14510	-0.14510				
$\cos\phi\sin^2\theta$	0.71015	0.71015	0.49518			
$\cos\phi\ (\cos^2\theta-\sin^2\theta)$	0.29430	0.29430	-4.80880e-002	0.42042		
$1/(\rho-\tau)^2$	1.00000	1.00000	-0.14510	0.71015	0.29430	
$\cot^2\theta$	0.67187	0.67187	0.52691	0.99714	0.41251	0.67187

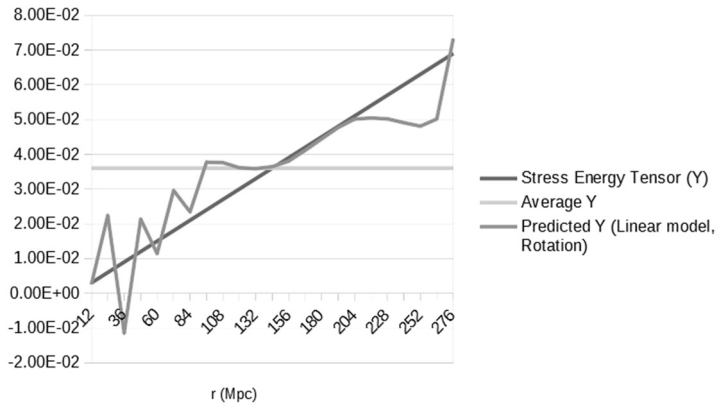

Fig. 4. Stress Energy Tensor and Predicted Dependent Variable (Linear, Rotation)

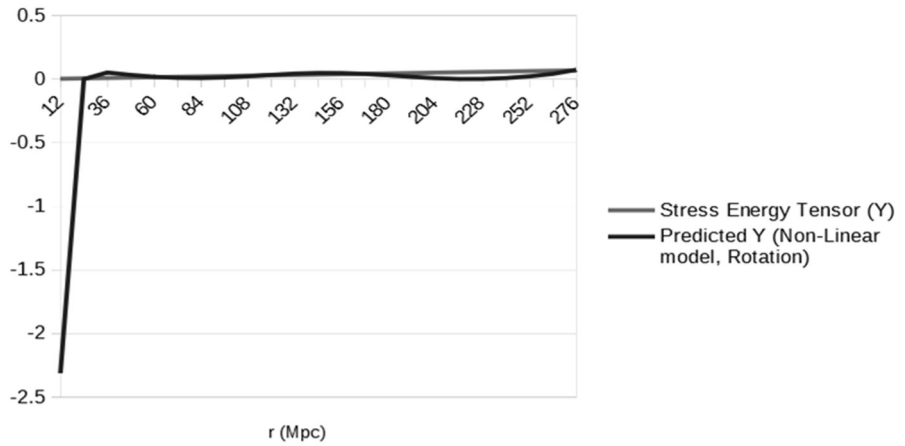

Fig. 5. Stress Energy Tensor and Predicted Dependent Variable (Non-linear, Rotation)

DISCUSSION INTERPRETATION OF THE NEGATIVE COEFFICIENTS

Negative coefficients are shown in Appendices from 2.1 to 2.4. The reasons are not identified yet, however possible reasons are:

1. Reflection or Scattering of Waves: A negative coefficient could indicate that some portion of the gravitational waves is being reflected or scattered back, rather than all the energy being absorbed or transmitted. This reflection could result in a negative pressure effect in the stress-energy tensor as perceived from the original propagation direction.

2. Wave's Destructive Interference: Gravitational waves can interfere constructively or destructively. The negative coefficient might represent regions where destructive interference occurs, reducing the net amplitude of the wave and thus appearing as a negative contribution in the stress-energy tensor.

3. Energy Flux and Rotation (Frame-Dragging Effects): In the presence of rotation, frame-dragging effects (also known as the Lense-Thirring effect) can alter the energy distribution and propagation of gravitational waves. This could lead to regions where the effective stress-energy contribution is negative due to the complex interactions between the wave and the rotating spacetime.

4. Centrifugal Effects: The rotation of the source or the spacetime might introduce centrifugal effects that could lead to a redistribution of energy in such a way that some components of the stress-energy tensor become negative.

SIGNIFICANCE OF θ IN THE MODEL

The statistical significance of the trigonometric terms involving θ (the angle in spherical coordinates) in both the non-rotating and rotating cases suggests that the angular dependence of gravitational waves is crucial. This aligns with the theoretical understanding of gravitational waves, which exhibit angular dependence due to the quadrupole nature of the source. In particular, NSBH systems emit gravitational waves with strong quadrupole moments, meaning the angular orientation of the source significantly influences the waveform. This explains why the trigonometric terms involving θ are statistically significant in the calculations presented in this report, as they capture the effect of the source's angular position on the gravitational wave signal.

CONCLUSIONS AND RECOMMENDATIONS

The tensor equation for gravitational waves presented in this study applies to strong curvature, whereas Dirac originally described it in the context of a weak gravitational field with a constant metric tensor. This study's novelty lies in its ability to trace the source of gravitational waves—such as merging binary compact objects – and simulate the potential spinning motion of the emission source. To model the spinning source, the singularity is eliminated by assuming spacetime distortion. The gravitational waves emitted from the spinning source are included in the simulation, taking into account the geometric configuration between GW200115 and the LIGO-Virgo observatories.

The simulation results indicate that the fitting of the gravitational waves' tensor deteriorates when the spin of the source is included. This suggests that the proposed tensor equation may not fully explain this phenomenon. Additionally, there are uncertainties in the observed data regarding the angle of the spinning axis and the orbital rotation cycle of the source objects, which this analysis has not accounted for.

However, the actual observed detection period of the gravitational wave event GW200115 spans merely 6 minutes (360 seconds) on January 15, 2020. To adapt the theoretical timescale for practical numerical simulation, we may re-scale the extensive light travel timescale to fit the brief detection window. This adjustment ensures the model accounts for the actual duration over which the gravitational waves were observed, rather than the total travel time from the source, which this report took into account. By focusing on the observation period, we may be able to simulate the gravitational wave's impact within the time frame during which it interacted with the detector, providing a pragmatic and relevant representation of the event.

It is important to note that the mathematical model employed in this study only accommodates the rotation of a single compact strong mass, such as a neutron star or a black hole. It is not designed to simulate the more complex dynamics of a neutron star-black hole (NSBH) system, which involves both orbital rotation and individual spin components from each object. Therefore, while the model successfully captures the rotational characteristics of individual massive objects, it does not fully account for the intricate behavior of a binary NSBH system like the one for GW200115.

Despite this limitation, this study provides a crucial step in the exploration of gravitational waves emitted by a rotating compact object. The findings offer a clear and useful mathematical framework for understanding the emission of gravitational waves from single compact masses, which is applicable to many other scenarios. This research offers a model for the general behavior of gravitational wave emissions and the impact of spin and rotation in strong gravitational fields.

As part of future work, the current model can be extended to better simulate binary systems, incorporating both the spin and orbital dynamics of NSBH mergers. Further refinement of the mathematical framework will involve expanding the tensor equations to capture two-body interactions and gravitational interactions between the neutron star and the black hole. Addressing these aspects will significantly enhance the ability to model complex gravitational wave sources and could provide a more comprehensive understanding of events like GW200115.

REFERENCE

1. P.A.M. Dirac, *General Theory of Relativity*. Florida University, New York: A Wiley-Interscience Publication, John Wiley & Sons, 1975, 69 p.
2. A.S. Goldberger, *A Course in Econometrics*. Harvard University Press,1991, 405 p.
3. "Observation of gravitational waves from two neutron star–black hole coalescences, The LIGO Scientific Collaboration, the Virgo Collaboration, and the KAGRA Collaboration," *LIGO Caltech*, 2021. Accessed on 25 June 2024. Available: https://www.ligo.caltech.edu/page/ligo-data
4. H. Goldstein, C.P. Poole, J.L. Safko, *Classical Mechanics*; 3rd Edition. Pearson Education, Inc., 2002, 646 p.
5. Christopher M. Hirata, "Lecture IV: Stress-energy tensor and conservation of energy and momentum," *Caltech (Tapir)*, October 7, 2011. Available: http://www.tapir.caltech.edu/~chirata/ph236/lec04.pdf
6. Y. Matsuki, P.I. Bidyuk, "Numerical Simulation of Gravitational Waves from a Black Hole, using Curvature Tensors," *System Research & Information Technology*, no. 1, pp. 54–67, 2020. doi: https://doi.org/10.20535/SRIT.2308-8893.2020.1.05
7. Y. Matsuki, P.I. Bidyuk, "Simulating angular momentum of gravitational field of a rotating black hole and spin momentum of gravitational waves," *System Research & Information Technology*, no. 1, pp. 7–20, 2021. doi: https://doi.org/10.20535/SRIT.2308-8893.2021.1.01
8. Y. Matsuki, P.I. Bidyuk, *A Course in Black Hole Simulation*. LAP LAMBERT Academic Publishing, 2021, 84 p.

Received 27.12.2024

Appendix 1. Curvature tensors of gravitational waves

$\mu = v = 0$ $\rho = \sigma = 1$ $\beta = 0, 1, 2, 3$	$g^{00}g_{11,00} = 4\left\{-\frac{2\mathrm{m}}{\mu}(\rho-\tau)^{-\frac{2}{3}}\right\}_{,\tau\tau} = 4\left\{-\frac{2\mathrm{m}}{\mu}(-1)(-\frac{2}{3})(\rho-\tau)^{\frac{-5}{3}}\right\}_{,\tau} = -\frac{80\mathrm{m}}{9\mu(\rho-\tau)^{\frac{8}{3}}}$, $g^{00}g_{22,00} = -\frac{16\mu^2}{9(\rho-\tau)^{\frac{2}{3}}}$, $g^{00}g_{33,00} = -\frac{16\mu^2}{9(\rho-\tau)^{\frac{2}{3}}}\sin^2\theta$
$\mu = v = 1$ $\rho = \sigma = 0$ $\beta = 0, 1, 2, 3$	$-g^{11}_{,0}g_{11,0} = \frac{16}{9(\rho-\tau)^2}$
$\mu = v = 1$ $\rho = \sigma = 1$ $\beta = 0$	$g^{11}g_{11,11} + g^{II}_{,I}(g_{11,1} - \frac{1}{2}g_{11,1}) + g^{II}_{,I}(g_{11,1} - \frac{1}{2}g_{11,1}) = \frac{2}{3(\rho-\tau)^2}$, $\frac{1}{2}g^{11}g_{00}g_{11,0}g_{11,01} = \frac{20m}{27\mu(\rho-\tau)^{\frac{11}{3}}}$, $\frac{1}{2}g^{11}g_{00,}g_{11,01}g_{11,0} = \frac{20\mathrm{m}}{27\mu(\rho-\tau)^{\frac{11}{3}}}$, $\frac{1}{2}g^{11}_{,1}g_{00}g_{11,0}g_{11,0} = \frac{-8\mathrm{m}}{27\mu(\rho-\tau)^{\frac{11}{3}}}$, $\frac{1}{2}g^{11}g_{00}g_{11,0}g_{11,0} = \frac{20m}{27\mu(\rho-\tau)^{\frac{11}{3}}}$, $\frac{1}{2}g^{11}g_{00}g_{11,01}g_{11,0} = \frac{20m}{27\mu(\rho-\tau)^{\frac{11}{3}}}$, $\frac{1}{2}g^{11}_{,1}g_{00}g_{11,0}g_{11,0} = \frac{-8\mathrm{m}}{27\mu(\rho-\tau)^{\frac{11}{3}}}$, $\frac{1}{2}g^{11}g_{00,1}g_{11,0}g_{11,0} = 0$
$\mu = v = 1$ $\rho = \sigma = 1$ $\beta = 1$	$g^{11}g_{11,11} = \frac{10}{9(\rho-\tau)^{-2}}$, $g^{II}_{,I}(g_{11,1} - \frac{1}{2}g_{11,1}) + g^{II}_{,I}(g_{11,1} - \frac{1}{2}g_{11,1}) = -\frac{4}{9(\rho-\tau)^2}$, $\frac{1}{2}g^{11}g_{11}g_{11,1}g_{11,11} = \frac{-40m^2}{27\mu^2(\rho-\tau)^{\frac{13}{3}}}$, $\frac{1}{2}g^{11}g_{11}g_{11,11}g_{11,1} = \frac{-40m^2}{27\mu^2(\rho-\tau)^{\frac{13}{3}}}$, $\frac{1}{2}g^{11}_{,1}g_{11}g_{11,1}g_{11,1} = \frac{16m^2}{27\mu^2(\rho-\tau)^{\frac{13}{3}}}$, $\frac{1}{2}g^{11}g_{11,1}g_{11,1}g_{11,1} = \frac{-8m^2}{27\mu^2(\rho-\tau)^{\frac{13}{3}}}$, $\frac{1}{2}g^{11}g_{11}g_{11,1}g_{11,11} = \frac{-40m^2}{27\mu^2(\rho-\tau)^{\frac{13}{3}}}$, $\frac{1}{2}g^{11}g_{11}g_{11,11}g_{11,1} = \frac{-40m^2}{27\mu^2(\rho-\tau)^{\frac{13}{3}}}$, $\frac{1}{2}g^{11}_{,1}g_{11}g_{11,1}g_{11,1} = \frac{16\mathrm{m}^2}{27\mu^2(\rho-\tau)^{\frac{13}{3}}}$, $\frac{1}{2}g^{11}g_{11,1}g_{11,11}g_{11,1} = \frac{-8m^2}{27\mu^2(\rho-\tau)^{\frac{13}{3}}}$
$\mu = v = 1$ $\rho = \sigma = 1$ $\beta = 2$	$g^{11}g_{11,11} + g^{II}_{,I}(g_{11,1} - \frac{1}{2}g_{11,1}) + g^{II}_{,I}(g_{11,1} - \frac{1}{2}g_{11,1}) = \frac{2}{3(\rho-\tau)^2}$
$\mu = v = 1$ $\rho = \sigma = 1$ $\beta = 3$	$g^{11}g_{11,11} + g^{II}_{,I}(g_{11,1} - \frac{1}{2}g_{11,1}) + g^{II}_{,I}(g_{11,1} - \frac{1}{2}g_{11,1}) = \frac{2}{3(\rho-\tau)^2}$

$\mu = v = 1$ $\rho = \sigma = 2, 3$ $\beta = 0, 1, 2, 3$	$g^{11}g_{22,11} = \frac{16\mu^3}{18m}$, $g^{11}g_{33,11} = \frac{8\mu^3}{9\mathrm{m}}\sin^2\theta$
$\mu = v = 2$ $\rho = \sigma = 0, 1, 3$ $\beta = 0, 1, 2, 3$	$-g^{22}_{,1}g_{22,0} = -\frac{40}{9(\rho-\tau)^2}$, $-g^{22}_{,1}g_{22,1} = \frac{40}{9(\rho-\tau)^2}$, $-g^{22}g_{33,22} = 8\cos^2\theta - 8\sin^2\theta$
$\mu = v = 3$ $\rho = \sigma = 0$ $\beta = 0, 1, 2, 3$	$-g^{33}_{,0}g_{33,0} = \frac{64}{9(\rho-\tau)^{-2}}$
$\mu = v = 3$ $\rho = \sigma = 1$ $\beta = 0, 1, 2, 3$	$-g^{33}_{,1}g_{33,1} = \frac{64}{9(\rho-\tau)^{-2}}$
$\mu = v = 3$ $\rho = \sigma = 2$ $\beta = 0, 1, 2, 3$	$-g^{33}_{,2}g_{33,2} = 16\cot^2\theta$

Note: All other components are 0.

Appendix 2. Estimated Coefficients, Standard Errors, *t*-statistics

2.1. No rotation, linear space time distortion (for equation (34) with the input data Table 2 Two models for simulating the distorted time-space - Case 2)

Dependent Variable: stress energy tensor

Independent Variable	**Estimated Coefficient**	**Standard Error**	***t*-statistic**	**Estimated Coefficient by SST manual mode**
$\frac{1}{(\rho-\tau)^2}$	-6.02704e-014	5.20397e-015	-11.58162	-6.02704e-014
$\frac{1}{(\rho-\tau)^{\frac{11}{3}}}$	1.37710e-024	1.46926e-025	9.37274	1.37710e-024
$\frac{1}{(\rho-\tau)^{\frac{13}{3}}}$	-3.97632e-031	4.84817e-032	-8.20170	-3.97632e-031
$\sin^2\theta$	0.10526	3.59601e-003	29.27186	0.10526
$\cos^2\theta - \sin^2\theta$	6.82777e-002	3.71969e-003	18.35576	6.82777e-002
$\cot^2\theta$	2.21982e-005	1.38632e-004	0.16012	2.21982e-005

Number of Observations	23
R-squared	0.95030
Corrected *R*-squared	0.93568
Sum of Squared Residuals	4.52692e-004
Standard Error of the Regression	5.16032e-003
Durbin–Watson Statistic	1.18063
Mean of Dependent Variable	3.60000e-002
R-squared by SST manual mode	0.95029
Durbin–Watson Statistic by SST manual mode	1.18067

2.2. Rotation, linear space time distortion (for equation (41) with the input data Table 2 Two models for simulating the distorted time-space - Case 2)

Dependent Variable: stress energy tensor

Independent Variable	Estimated Coefficient	Standard Error	*t*-statistic	Estimated Coefficient by SST manual mode
$\cos\varphi \frac{1}{(\rho-\tau)^2}$	3.82906e-014	3.10774e-014	1.23211	3.82906e-014
$\cos\varphi \frac{1}{(\rho-\tau)^{\frac{11}{3}}}$	2.56705e-025	7.38201e-025	0.34774	2.56705e-025
$-\cos\varphi \frac{1}{(\rho-\tau)^{\frac{13}{3}}}$	-5.28814e-031	1.04920e-031	-5.04016	-5.28814e-031
$\cos\varphi \sin^2\theta$	-5.09843e-002	5.09539e-003	-10.00596	-5.09843e-002
$\cos\varphi(\cos^2\theta-\sin^2\theta)$	-9.87054e-003	8.15690e-003	-1.21008	-9.87054e-003
$\frac{1}{(\rho-\tau)^2}$ *	-4.75441e-014	1.08187e-014	-4.39461	-4.75441e-014
$\cot^2\theta$ *	5.17654e-002	5.10418e-003	10.14176	5.17654e-002

* These components are on the axis of the rotation and belong to W_{33}; therefore, cosϕ is not multiplied.

Number of Observations	23
R-squared	0.78633
Corrected *R*-squared	0.70621
Sum of Squared Residuals	1.94607e-003
Standard Error of the Regression	1.10286e-002
Durbin–Watson Statistic	1.87168
Mean of Dependent Variable	3.60000e-002
R-squared calculated by SST manual mode	0.80481
Durbin–Watson Statistic by SST manual mode	1.88005

2.3. No rotation, non-linear spacetime distortion (for equation (34) with the input data Table 2 Two models for simulating the distorted time-space - Case 1)

Dependent Variable: stress energy tensor

Independent Variable	Estimated Coefficient	Standard Error	*t*-statistic	Estimated Coefficient by SST manual mode
$\frac{1}{(\rho-\tau)^2}$	1.22587	0.32131	3.81529	1.20947
$\frac{1}{(\rho-\tau)^{\frac{11}{3}}}$	-5.37506e-005	1.40882e-005	-3.81530	-5.30312e-005
$\frac{1}{(\rho-\tau)^{\frac{13}{3}}}$	-0.68259	4.58014e-002	-14.90334	-0.68105
$\sin^2\theta$	0.26481	1.38169e-002	19.16566	0.26428
$\cos^2\theta-\sin^2\theta$	0.13871	8.71783e-003	15.91077	0.13834
$\cot^2\theta$	1.07687e-003	5.27743e-004	2.04052	1.10100e-003

Number of Observations	23
R-squared	0.95736
Corrected *R*-squared	0.94481
Sum of Squared Residuals	3.88397e-004
Standard Error of the Regression	4.77984e-003

Durbin–Watson Statistic	0.75429
Mean of Dependent Variable	3.60000e-002
R-squared calculated by SST manual mode	0.95777
Durbin–Watson Statistic calculated by SST manual mode	0.76027

2.4. Rotation, non-linear spacetime distortion (for equation (41) with the input data Table 2 Two models for simulating the distorted time-space - Case 1)

Dependent Variable: stress energy tensor

Independent Variable	**Estimated Coefficient by SST manual mode**
$\cos\varphi \frac{1}{(\rho-\tau)^2}$	-7.95519
$\cos\varphi \frac{1}{(\rho-\tau)^{\frac{11}{3}}}$	1.09155e-004
$-\cos\varphi \frac{1}{(\rho-\tau)^{\frac{13}{3}}}$	-1.77473e-002
$\cos\varphi \sin^2\theta$	2.32505e-003
$\cos\varphi(\cos^2\theta-\sin^2\theta)$	4.55818e-002
$\frac{1}{(\rho-\tau)^2} *$	5.28200
$\cot^2\theta *$	5.48484e-004

R-squared calculated by SST manual mode	6.05462e+002
Durbin–Watson Statistic calculated by SST manual mode	0.32756

INFORMATION ON THE ARTICLE

Yoshio Matsuki, ORCID: 0000-0002-5917-8263, National University of Kyiv Mohyla Academy, Ukraine, e-mail: matsuki@wdc.org.ua

РЕГРЕСІЙНИЙ АНАЛІЗ СПОСТЕРЕЖЕНЬ LIGO-VIRGO WG200115 ІЗ ВИКОРИСТАННЯМ ТЕНЗОРІВ КРИВИЗНИ З РІВНЯНЬ ЕЙНШТЕЙНА ТА ГРАВІТАЦІЙНИХ ХВИЛЬ ДІРАКА / Й. Мацукі

Анотація. Подано математичне виведення тензорів кривизни з розв'язку Шварцшильда для гравітаційного поля разом із виведенням гравітаційних хвиль як другої похідної поля. Усунення горизонту подій є основним внеском цієї статті, яка ґрунтується на підході Пола Дірака в його книзі 1975 року «Загальна теорія відносності». Представлено лінійні та нелінійні моделі для функції викривлення простору-часу. Відповідність тензорного рівняння для гравітаційних хвиль перевіряється з використанням геометричної інформації зі спостережень LIGO-Virgo WG200115 із застосуванням економетричних методів із такими індикаторами, як *R*-квадрат надійності даних і відповідність моделі розподілу даних, а також статистики Дарбіна–Ватсона для передбачуваності часових рядів. Результати показують хорошу відповідність отриманої математичної моделі спостережуваній геометрії. Різні моделі для моделювання викривлення простору-часу демонструють різний ступінь відповідності спостережуваній геометрії, при цьому менш спотворена модель забезпечує краще пояснення спостережуваних гравітаційних хвиль. Узгодженість моделі зменшується, якщо враховувати обертання об'єкта-джерела, хоч нейтронної зірки, хоч чорної діри. Необхідні подальші зусилля з моделювання, щоб точно представити процес злиття чорних дір (NSBH) і його роль у формуванні гравітаційних хвиль.

Ключові слова: тензори кривизни, рішення Шварцшильда, гравітаційні хвилі, горизонт подій, спостереження LIGO-Virgo.